Water balance modelling in a tropical watershed under deciduous forest (Mule Hole, India): Regolith matric storage buffers the groundwater recharge process

Laurent Ruiz, M.R.R. Varma, M.S. Mohan Kumar, Muddu Sekhar, Jean-Christophe Maréchal, Marc Descloitres, Jean Riotte, Sat Kumar, C. Kumar, Jean-Jacques Braun

Water balance modelling in a tropical watershed under deciduous forest (Mule Hole, India) : regolith matric storage buffers the groundwater recharge process

Laurent Ruiz[a,b,*], Murari R. R. Varma[c,d], M. S. Mohan Kumar[c,d], M. Sekhar[c,d], Jean-Christophe Maréchal[c,e,f,g], Marc Descloitres[c,h] Jean Riotte[c,e,f,g] and Jean-Jacques Braun[c,e,f,g]

[a] INRA, UMR1069, Sol Agro et hydrosystème Spatialisation, 35000 Rennes, France

[b] Agrocampus Ouest, UMR1069, Sol Agro et hydrosystème Spatialisation, 35000 Rennes, France

[c] Indo-French Cell for Water Sciences, IISc-IRD Joint laboratory, Indian Institute of Science, 560012 Bangalore, India

[d] Indian Institute of Science, Department of Civil Engineering, , Bangalore 560 012, INDIA

[e] Université de Toulouse ; UPS (OMP) ; LMTG; 14 Av Edouard Belin, F-31400 Toulouse, France

[f]CNRS ; LMTG ; F-31400 Toulouse, France

[g]IRD ; LMTG ; F-31400 Toulouse, France

[h] IRD ; Université de Grenoble ; CNRS ; LTHE , BP53, 38041 Grenoble, Cedex 9, France

[*] corresponding author:

Laurent RUIZ, INRA, Sol Agro and hydroSystemes, 4 rue Stang Vihan, F-29000 Quimper, France

E-mail : ruiz@rennes.inra.fr

Tél : +33 (0) 2 98 95 99 64

Abstract

Accurate estimations of water balance are needed in semi-arid and sub-humid tropical regions, where water resources are scarce compared to water demand. Evapotranspiration plays a major role in this context, and the difficulty to quantify it precisely leads to major uncertainties in the groundwater recharge assessment, especially in forested catchments. In this paper, we propose a lumped conceptual model (COMFORT), which accounts for the water uptake by deep roots in the unsaturated regolith zone. The model is calibrated using a five year hydrological monitoring of an experimental watershed under dry deciduous forest in South India (Mule Hole watershed).

The model was able to simulate the stream discharge as well as the contrasted behaviour of groundwater table along the hillslope. Water balance simulated for a 32 year climatic time series displayed a large year-to-year variability, with alternance of dry and wet phases with a time period of approximately 14 years. On an average, input by the rainfall was 1090 $mm.year^{-1}$ and the evapotranspiration was about 900 $mm.year^{-1}$ out of which 100 $mm.year^{-1}$ was uptake from the deep saprolite horizons. The stream flow was 100 $mm.year^{-1}$ while the groundwater underflow was 80 $mm.year^{-1}$.

The simulation results suggest that i) deciduous trees can uptake a significant amount of water from the deep regolith, ii) this uptake, combined with the spatial variability of regolith depth, can account for the variable lag time between drainage events and groundwater rise observed for the different piezometers, iii) water table response to recharge is buffered due to the long vertical travel time through the deep vadose zone, which constitutes a major water reservoir.

50 This study stresses the importance of long term observatories for the understanding of
51 hydrological processes in tropical forested ecosystems.
52
53 **Key Words**: matric porosity, groundwater recharge, lumped model, semi-arid tropics,
54 evapotranspiration, vadose zone, forested watershed hydrology.
55
56 **Introduction**
57
58 Accurate assessment of water balance at the watershed scale is of major importance in a
59 context of a global dramatic increase of human demand for water, either for urban or
60 agricultural requirements. This assessment is complex, since water balance results from the
61 interaction of climate, geology, morphology, soil and vegetation (De Vries and Simmers,
62 2002).
63 A large suit of rainfall-runoff models are available that are either fully empirical or
64 mechanistic, which make it possible to predict with reasonable accuracy water balance from
65 watersheds in temperate climates (Beven, 2001 ; Wagener et al., 2004). These models are
66 usually evaluated according to their ability to simulate stream discharge. In semi-arid or arid
67 climates, calibration of watershed models is difficult because streams are often ephemeral.
68 Moreover, as potential evapotranspiration equals or surpasses average precipitation, a correct
69 evaluation of actual evapotranspiration becomes crucial (Scanlon et al., 2002, 2006 ; Sekhar
70 et al., 2004 ; Anuraga et al., 2006). Despite the large amount of work dedicated to assess
71 evapotranspiration at the watershed scale, this flux remains the largest source of uncertainity
72 in water budgeting, especially in the case of forested watersheds (Zhang et al., 2001; 2004).
73

The objective of this paper is to propose a methodology for water balance estimation in a tropical forested watershed, based on the calibration of a conceptual model against stream discharge and groundwater level data. The experimental watershed used in this study was developed as part of the project "Observatoire de Recherche en Environnement – Bassin Versant Expérimentaux Tropicaux" (http://www.ore.fr/) (Braun et al., 2005). Our results show that the deep vadose zone plays a major role in buffering the groundwater response to the water percolation.

Site description

The study site is situated in South India (Figure 1), at 11° 44' N and 76° 27' E (Karnataka state, Chamrajnagar district).

Figure 1: Location map of the experimental site

It is located in the transition zone of a steep climatic and geomorphologic gradient at the edge of the rifted continental passive margin of the Karnataka Plateau, which was the focus of extensive geomorphologic studies (Gunnell and Bourgeon, 1997). This plateau, developed on the high-grade metamorphic silicate rocks of the West Dharwar craton (Moyen et al., 2001), is limited westward by the Western Ghâts, a first order mountain range. This mountain forms an orographic barrier, inducing an steep climatic gradient, with annual rainfall decreasing from west to east from about 6000 mm to 500 mm within a distance of about 80 km (Pascal, 1982). These Ghâts are of critical ecological and economical importance and also an important source of all major South Indian rivers, flowing eastward towards the Gulf of Bengal. The climatic transition zone is mainly covered by dry deciduous forests, belonging to

the wildlife sanctuaries of Mudumalai, Waynad, Bandipur and Nagarahole (Prasad and Hedge, 1986). Such a tropical climosequence is comparable, although much steeper (Gunnell, 2000), to the well documented monsoonal West African and the Northeast Brazilian climosequences (Gunnell, 1998).

The Mule Hole experimental watershed (4.1 km^2) is located in the climatic semi-humid transition area and the mean annual rainfall (n = 25 years) is 1120 mm. The mean yearly temperature is 27 °C. On the basis of the aridity index defined as the ratio of mean annual precipitation to potential evapotranspiration, the climate regime can be classified as humid (UNESCO, 1979). Nevertheless, the climate is characterized by the occurrence of a marked dry season (around 5 months from December to April) and by recurrent droughts, depending on the monsoon rainfalls. The rainfall pattern is bimodal, as it is affected by both the South West Monsoon (June to September) and the North East Monsoon (October - December) (Gunnell and Bourgeon, 1997). Streams are ephemeral, and their flow duration ranges from a few hours to a few days after the storm events.

The watershed is mostly undulating with gentle slopes and the elevation of the watershed ranges from 820 to 910 m above sea level (Figure 1). The morphology of the watershed is convexo-concave highly incised by the temporary stream network. The lithology, representative of the West Dharwar craton (Naqvi and Rogers, 1987), is dominated by complexly folded, heterogeneous Precambrian peninsular gneiss intermingled with mafic and ultramafic rocks of the volcano-sedimentary Sargur series (Shadakshara Swamy et al., 1995). The Peninsular gneiss represents at least 85% of the watershed basement and the average strike value is N80°, with a dip angle ranging from 75° to the vertical (Descloitres et al., 2008). In such hard-rock context, the aquifer can generally be divided into two parts: one

upper part is the porous clayey to loamy regolith with an apparent density lower than the rock bulk density, the other is in the fractured-fissured protolith with an apparent density close to the bulk density of the rock and a network of fractures of a density decreasing with depth (Sekhar et al., 1994, Maréchal et al., 2004 ; Wyns et al., 2004 ; Dewandel et al., 2006). In the Mule Hole watershed, the average depth of the regolith is 17 m, as estimated through an extensive geophysical and geochemical survey (Braun et al., 2006 ; Braun et al., 2008). The distribution of the regolith depth (Figure 2) shows that the range of variation is 5 to 27 m. No correlation with the position on the hillslope was found. Average total porosity of the regolith is around 12%. Magnetic Resonance Sounding (MRS) performed on the watershed (Legchenko et al., 2006) showed that drainage porosity is around 1% in the regolith and below the detection level (<0.5%) in the fractured rock. Finally, timelapse geophysical measurements of both ERT and MRS conducted at the outlet of the watershed indicated a seasonal infiltration of water under the stream (Descloitres et al., 2008). A hydrological investigations allowed estimating the indirect recharge from the stream at around 30 $mm.year^{-1}$ at the watershed scale (Maréchal et al., 2009).

Figure 2 : distribution of regolith depth across the Mule Hole watershed (from a geophysical and geochemical survey by Braun et al., 2008)

The soil distribution in the watershed was determined by Barbiéro et al. (2007). The gneissic saprolite, cohesive to loose sandy, crops out both in the streambed and at the mid-slope in approximately 22% of the watershed area. The lower part of the slope and the flat valley bottoms (12% of the area) are covered by black soils (Vertisols and Vertic intergrades), which are 2 m deep on an average. Shallow red soils (Ferralsols and Chromic Luvisols), which are of 1 to 2 m deep, cover 66% of the entire watershed area. The watershed is covered by a dry

149 deciduous forest with different facies linked to the soil distribution (Barbiéro et al., 2007).
150 Minimal human activity is present as it belongs to the Bandipur National Park, dedicated to
151 wildlife and biodiversity preservation. The predominent tree component of the vegetation
152 consists of *Anogeissus-Terminalia-Tectona* association (ATT facies) forming a relatively
153 open canopy not exceeding 20 m (Prasad and Hedge, 1986 ; Pascal, 1986). Phenology is
154 marked by a strong seasonality, with leaf senescence starting in December and leaf flushing
155 occurring in early April, one or two month before the first significant monsoon rains. This
156 surprising behaviour, leading to a deciduous period of only 2-3 months, much shorter than the
157 dry season, is a general feature of the Asian forests (Singh and Kushawaha, 2005), and was
158 quoted as the "paradox of Asian monsoon forest" by Elliot et al. (2006).
159
160 **Model description**
161
162 The model COMFORT (**CO**nceptual **M**odel for hydrological balance in **FOR**es**T**ed
163 catchments) proposed in this article allows simulating the daily water budget of a forested
164 watershed, through a simple and widely accepted conceptual description of the hydrological
165 processes. It includes a lumped model for the soil moisture and the evapotranspiration in the
166 forest (Granier et al., 1999), a surface runoff model based on the variable source area theory
167 (Moore et al., 1983 ; Beven, 2001) and linear reservoirs for the recharge and groundwater
168 discharge (Beven, 2001 ; Putty and Prasad, 2000). Its originality relies on the introduction of
169 an additional water reservoir located in the weathered vadose zone (saprolite) below the soil,
170 accessible to tree roots but not to understorey vegetation roots.
171
172 ***Figure 3 : A schematic representation of the model COMFORT***
173

The model includes two modules, calibrated and run successively (Figure 3): the first one is a slightly modified and simplified version of the lumped water balance model presented by Granier et al (1999), which simulates the daily water balance for the forested soil and the surface runoff Q_s, while the second one simulates the flow of water through the deep vadose zone and the groundwater flow. Forcing variables are the daily rainfall (Rf), the Penman potential evapotranspiration (PET), and the forest leaf area index (LAI). The details of each of these modules is given below.

Module 1: Soil moisture

This module computes the daily variations in the soil moisture deficit (SMD, in mm) as:

$$\Delta SMD = E_{In} + T + E_u + PR + Q_s - Rf$$

and

$$0 < SMD < SMD_{max}$$

with E_{In} ($mm.day^{-1}$) being the evaporation of rainfall intercepted by the forest canopy, T ($mm.day^{-1}$) the tree transpiration, E_u ($mm.day^{-1}$) the evapotranspiration of the understorey layer, PR ($mm.day^{-1}$) is the percolation below the soil layer, also called "potential recharge" by De Vries and Simmers (2002), Q_s ($mm.day^{-1}$) the surface runoff, Rf ($mm.day^{-1}$) the rainfall and SMD_{max} (mm) the maximum soil water deficit, equivalent to the soil water holding capacity.

The throughfall ($Rf - E_{In}$) on the saturated area of the watershed (SA in %) reaches the stream as surface runoff (Q_s in $mm.day^{-1}$) :

$$Q_s = (Rf - E_{In}) \times SA / 100$$

Saturated area is usually computed as a function of water storage in the soil and the groundwater (see for example Putty and Prasad, 2000). In our context, groundwater level is far below the ground level, thus SA is modelled as an exponential function of the soil moisture deficit:

$$SA = SA_{max} \times \exp (- a \times SMD)$$

with SA_{max} the maximal extension of the saturated area (%), and a being the exponent constant. The proportion (%) of the soil surface covered by tree leaves (ε) is calculated from the forest LAI with the Beer-Lambert function assuming a light coefficient of extinction of 0.5 (Granier et al. 1999).

$$\varepsilon = 1 - e^{- 0,5 \times LAI}$$

The evaporation of rainfall intercepted by the forest canopy, or interception losses, E_{In} ($mm.day^{-1}$) is computed as:

$$E_{In} = \text{minimum} (\varepsilon \times Rf ; \varepsilon \times PET ; \varepsilon \times In)$$

with In (mm) the canopy storage capacity. This equation implies that canopy cannot store water for more than one day, and thus interception losses are nil during non rainy days. This simplification is justified by the fact that In is generally smaller than PET at a daily time step.

As proposed by Granier et al. (1999), to account for the fact that the rate of evaporation of intercepted water is approximately four time greater than transpiration rate (Rutter, 1967), PET is reduced by 20 % of the amount of intercepted water and the total actual evapotranspiration (AET) is limited to 1.2 × PET. The tree transpiration from the soil layer (T_s in $mm.day^{-1}$) is then calculated as:

$$T_s = \text{minimum}\ (SMD_{max} - SMD\ ;\ (\varepsilon \times PET) - (0{,}2 \times E_{In})\ ;\ 1.2 \times PET - E_{In})$$

with SMD_{max} the maximum soil water deficit (mm), equivalent to the soil water holding capacity. In their model, Granier et al. (1999) propose that T/PET ratio decreases linearly when soil moisture reaches a critical level of 40% of the water holding capacity of the soil. In our model, for the sake of simplicity, transpiration is only limited by the amount of water present in the soil reservoir.

Evapotranspiration from understorey vegetation is calculated as:

$$E_u = \text{minimum}\ (SMD_{max} - SMD - T_s\ ;\ (1-\varepsilon) \times PET\ ;\ 1.2 \times PET - T_s - E_{In})$$

Actual evapotranspiration from the soil layer (AETs in $mm.day^{-1}$) is then:

$$AET_s = E_{In} + T_s + E_u$$

Eventually, the water in excess in the soil reservoir (when SMD<0) percolates below the soil layer, as "potential recharge" (PR in $mm.day^{-1}$). This flow is an input to the weathered zone reservoir (module 2).

Module 2: Weathered zone and groundwater

This module simulates the daily variations of the moisture deficit in the weathered zone (WZMD in mm) as :

$$\Delta WZMD = T_{WZ} + R - PR$$

where T_{WZ} is the tree transpiration from the weathered zone below the soil ($mm.day^{-1}$), PR the potential recharge calculated in the module 1 ($mm.day^{-1}$) and R ($mm.day^{-1}$) the recharge. The potential evapotranspiration from the weathered zone ($mm.day^{-1}$) is the residual of the potential transpiration of trees minus the actual tree transpiration in the soil zone:

$$PET_{WZ} = \varepsilon \times PET - (0{,}2 \times E_{In}) - T_s$$

The actual transpiration from the weathered zone T_{WZ} ($mm.day^{-1}$) is then:

$$T_{WZ} = \text{minimum}\ (WZMD_{max} - WZMD\ ;\ PET_{WZ})$$

with $WZMD_{max}$ (mm) the maximum water deficit of the weathered zone.

Recharge (R_{WZ} in $mm.day^{-1}$) is the water in excess in the weathered zone (when WZMD<0). To account for the observed smoothness of the recharge process, R_{WZ} is directed to a recharge reservoir R (mm), and the effective recharge (R_{GW} in $mm.day^{-1}$) reaching the groundwater reservoir (GW in mm) is calculated as :

$$R_{GW} = \alpha_1 \times R$$

with α_1 (day^{-1}) the recession coefficient of the recharge reservoir R.

Eventually, the daily variation of water content in the groundwater reservoir (GW in mm) is calculated as:

$$\Delta GW = R_{GW} - Q_{GW}$$

with the Q_{GW} the groundwater flow ($mm.day^{-1}$) calculated as :

$$Q_{GW} = \alpha_2 \times GW$$

with α_2 (day^{-1}) the recession coefficient of the groundwater reservoir GW. As the groundwater level is always deeper than the stream bed at the outlet, this flow is considered as an underflow.

The groundwater table level (L_{GW} in meters above sea level) is then calculated as:

$$L_{GW} = L_0 + GW/(Sy \times 1000)$$

297

298 with L_0 (masl) the altitude of the base of the aquifer and Sy its specific yield.

299

300 **Data acquisition and model calibration procedure**

301

302 The climatic data (daily rainfall and PET) necessary to run the model were available for the
303 period 2003-2007 from the automatic weather station (CIMEL, type ENERCO 407 AVKP)
304 installed at the Mulehole forest check post, which is 1.5 km West to the watershed outlet
305 (Figure 1). Daily rainfall data were available at the same location from 1976 to 1995 from
306 Indian Meteorological Department. Daily rainfall data were also available from the
307 Ambalavayal weather station, located 20 km west of the study site, for the years 1979 to
308 2004. As statistical analysis showed a strong correlation between the two stations, the seven
309 missing years (1996-2002) in the Mule Hole were inferred from the Ambalavayal data.
310 Granier at al. (1999) have shown that soil water content can be equally simulated in forest
311 stands under different climates either with models based on Penmann potential
312 evapotranspiration or with mechanistic approaches tacking into account the canopy structure.
313 Although many studies have shown that evapotranspiration is greater from forest than for the
314 short size vegetation (Zhang et al., 2001) this difference is mainly attributed to better access
315 to soil water at depth. Thus Penmann potential evapotranspiration was used as a forcing
316 variable to the model.

317

318 As year to year variations in PET were little during the years 2003 to 2007, an average daily
319 PET series was calculated and applied to the period 1976-2002. Using an average annual
320 curve of PET does not affect much the rainfall-runoff models (Burnash, 1995 ; Oudin et al.,
321 2005). The simulations were run on the reconstructed time series 1976-2007. Stream

322 discharge (Q_s) is measured since August 2003 at a 6 minutes time step using a flume built at
323 the outlet of the watershed. Due to technical problems, level recording was not available from
324 15th April 2007 to 7th August 2007. A set of 13 observation wells were drilled in the area in
325 2003 (P1-P6) and 2004 (P7-P13) (Figure 1). Most of these wells are dedicated to the
326 monitoring of the effects of water seepage from the stream. Wells P2, P3, P5, P6, P9 and P10
327 are not influenced by the indirect recharge from the stream (Maréchal et al., 2009), and can be
328 used to assess the direct recharge. The water levels are monitored in all the wells either
329 manually at a monthly time step or automatically at an hourly time-step. Due to technical
330 problems (among which elephant attacks), P2 and P9 didn't give reliable records and were not
331 included in the analysis. Additional data from an observation well (OW9) monitored by the
332 Department of Mines and Geology (Karnataka State) since 1975, and located 20 km east of
333 the watershed, which is close to the forest border, was used in the analysis.
334
335 As no measurement of forest leaf surface were carried out in the watershed, the evolution of
336 LAI was hypothesised from qualitative observations from the site and references from
337 literature concerning local tree phenology (Prasad and Hedge, 1986 ; Sundarapandian et al.,
338 2005) and NDVI records for Indian forests (Prasad et al., 2005). Seasonality of leaf flushing
339 and senescence is mostly driven by photoperiod, and therefore can be taken as a constant from
340 one year to the other (Elliot et al., 2006 ; Singh and Kushwaha, 2005). The proposed LAI
341 pattern is presented in the Figure 4a along with ε variations. The comparison with the average
342 monthly rainfall and PET over 32 years period (Figure 4b) shows that maximum PET is
343 reached during the deciduous period and that on average, rainfall exceeds PET during five
344 months.
345

Figure 4: a) daily forest LAI and coefficient of extinction ε, b) average monthly rainfall (Rf) (1976-2007) and PET (2003-2007). Vertical bars indicate standard deviation of Rf.

The two modules were run and calibrated successively, and the model performance was assessed using the Nash & Sutcliffe (1970) efficiency criterion. The module 1 is calibrated against the observed stream discharge values. This module has three forcing variables (Rf, PET and LAI) and four parameters (In, a, SA_{max} and SMD_{max}). As the sensitivity analysis showed that the model was little sensitive to In value, it was set at 1 mm and calibration was performed on the three remaining parameters. The time series obtained for the potential evapotranspiration from the weathered zone (PET_{WZ}) and the potential recharge (PR) are then used as forcing variables for the module 2, which includes five parameters ($WZMD_{max}$, α_1, α_2, Sy and L_0). The module 2 is calibrated for each piezometer against observed water table levels. To minimize equivalence possibilities, the following procedure was adopted: because $WZMD_{max}$ determines the date of initial water table rise, it is first adjusted by trial and error; then the four remaining parameters are automatically calibrated, with Sy values constrained smaller than 0.01, according to the conclusions of MRS survey (Legchenko et al., 2006). For each calibration, the solver was run with contrasting sets of initial parameter values, which later converged towards the same solution.

Results

Figure 5: observed (black line) and simulated (grey line) daily surface runoff (Qs in $mm.day^{-1}$) at the Mule Hole watershed outlet for the 5 years of monitoring. Secondary axis is daily rainfall (Rf) in mm.

371 The Figure 5 compares the observed and the simulated surface runoff (Q_s) at the Mule Hole
372 watershed outlet for the 5 years of monitoring. The Nash-Sutcliffe parameter calculated using
373 the monthly values is 74. Despite this relatively low value, the model was able to reproduce
374 the general trend of observed runoff, in particular the delay between the first monsoon rains
375 and the first observed stream runoff. On the other hand, it was unable to reproduce the runoff
376 observed after summer storm events in 2005, because they are due to Hortonian flow, a
377 mechanism that was not accounted for in the model. However, this kind of event is of
378 marginal importance in this pedoclimatic context. Considering that rainfall is measured in
379 only one weather station located outside the watershed and the high spatial variability of
380 rainfall, especially during strong individual storms, a perfect fit was not expected. In
381 particular in 2005, two events, on 22nd of October and 4th of November, produced 34 mm.day^{-1}
382 and 20 mm.day^{-1} of runoff for rains of 52 mm.day^{-1} and 28 mm.day^{-1} respectively. For these
383 events, the actual rainfall in the watershed was probably much higher than the measured one.
384 This is likely to have affected the assessment of water balance for the year 2005, as these two
385 storms represent about one quarter of the total yearly runoff. However, this kind of event
386 remains very rare: during the five monitoring years, only these two events produced more
387 than 20mm of runoff, and only five other individual events produced more than 10 mm of
388 runoff.
389
390 The calibrated parameter values are: a = 0.1, SA_{max} = 33.3% and SMD_{max} = 173 mm. The
391 value of maximal saturated area is probably overestimated, considering that the flat valley
392 bottom overlaid by black soil occupies about 12% of the watershed area. The two exceptional
393 storm events mentioned above played an important role in this overestimation. The calibrated
394 value of SMD_{max} is consistent with the soil moisture monitoring carried out in 2004 and 2005

395 in the site, showing a maximum variation of volumetric water content of 7% in red and black
396 soils (Barbiéro et al., 2007) and an average 2 m depth (Braun et al., 2006).
397
398 ***Table 1 : Soil water balance (mm.year^{-1}) for the monitored year and yearly average for the***
399 ***monitored period and the whole 32 year simulated period. Signification of terms is in the***
400 ***text. *2003-2006 average***
401
402 Annual soil water balances as well as averages for the monitoring period and the 32 years
403 simulation period are presented in the Table 1. Evapotranspiration is the most important sink
404 for water, accounting for about 70% of rainfall. Interception is about 10% of rainfall, which is
405 in the range of references values given in the literature for broad leaved forests (Ward and
406 Robinson, 2000). Potential recharge is large (197 mm.year^{-1} on the whole period), and
407 displays an important year to year variability. It is larger than the estimate based on the
408 regression equation proposed by Rangarajan and Athavale (2000) from tritium injection
409 experiments in granitic areas in India, which gives a value of about 150 mm.year^{-1} for the
410 conditions of Mule Hole. This difference might be due to specificities of the study site, in
411 particular the relatively low PET, mainly due to low temperatures linked with the altitude and
412 to the forested environment which contributes to decrease soil compaction and increase
413 infiltration potential (Bruijnzeel, 2004; Ilstedt et al., 2007). Results also show that the
414 monitoring period is quite representative of the whole 32 years period with respect to the soil
415 water balance.
416
417 ***Figure 6 : relative variation of water table level in hillslope piezometer, compared to***
418 ***simulated potential recharge. Reference values for water table depth are 16.8 m, 27.8 m,***
419 ***39.1 m and 37.4 m for P10, P3, P5 and P6 respectively.***

The Figure 6 compares the simulated daily potential recharge with observed relative variations in the water table level in hillslope piezometers. Although all piezometers showed a consistent global tendency to water level rise, they displayed significant contrasted behaviour. The relatively shallow piezometer (P10) responded each year to recharge, and the water level rise was almost simultaneous with the first occurrence of the potential recharge. Then the water level variation pattern was smooth, and the yearly maximum level was reached each year about two months after the end of the potential recharge period. For P3, the water table level did not increase in 2004, however showed a steep increase at the end of the 2005 rainy season, followed by a gentle continuous increase. In this well, ephemeral water table variations suggest the occurrence of some preferential flow (from August to October in 2006 and 2007). Finally, the deep piezometers P5 and P6 displayed a declining tendency in 2004 and 2005, a stabilisation or a very gentle rise in 2006, and a marked rise at the end of the rainy season 2007. These contrasted patterns of water table variation among the different hillslope piezometers suggest that they are linked with local processes and not by a regional aquifer dynamics.

Figure 7: Observed (dots) and simulated (lines) water level (in meter above sea level) in piezometer P3, P5 and P10 for the monitoring period.

Table 2 : Model parameters for the 3 simulated piezometers.

Comparison of the observed and the simulated water level variations in piezometers for the monitoring period show a very good agreement (Figure 7), with Nash criteria values of 96.7, 94.1 and 95.0 for P10, P3 and P5 respectively. Calibrated parameters (Table 2) are relatively

445 similar for the three piezometers. The most contrasted parameter is $WZMD_{max}$, the maximum
446 water deficit of the weathered zone, because it accounts for the observed very long lag-time
447 between water table rise observed in P10 in comparison with P3 (more than one year) and
448 with P5 (more than 3 years). The calibrated value of the specific yield is consistent with the
449 values obtained in similar fractured rock context in the region (Sekhar et al. 2004 ; Sekhar and
450 Ruiz, 2006 ; Maréchal et al., 2006).
451
452 The most surprising result is the small value of the recession coefficient of the recharge
453 reservoir (α_1). The recharge flow reaching the groundwater table is then very smooth, and it is
454 mostly compensated by the groundwater discharge. The consequence is that the variations in
455 the water content of the deep vadose zone (regolith and recharge reservoirs) are very large,
456 with a maximum range of variation for the entire 32 year period of 650 mm, 745 mm and 851
457 mm for P10, P3 and P5 respectively. Although very large, these variations are compatible
458 with the material porosity, considering the depth of this vadose zone (from 15 m to 40 m).
459
460 ***Figure 8 : Simulated variations of water table level (in masl) in piezometer P3, P5 and P10***
461 ***for the 32 year simulation period (lines). Dots represent observed values.***
462
463 ***Table 3: Watershed balance components (in mm.year^{-1}) for the piezometers P10, P3 and***
464 ***P5, for the monitoring period and the 32 year simulation and average watershed balance***
465 ***components calculated by weighted average (see text) .***
466
467 Average water balances components for each piezometer during the monitoring period and
468 the 32 years simulation period are presented in the Table 3. Unlike the observations for the
469 soil water balance, the monitored period appears dryer than the entire period. This is due to

the fact that the effects of the drought period from 2001 to 2003 persist longer at depth, which is apparent from the late rising of the deepest piezometers. The simulated long term variations of piezometers (Figure 8) reveals an alternance of wet and dry phases, of 12-15 years duration period. Maximum level in P5 is reached 2 to 3 years later than in P10. This simulated pattern was compared to the data recorded by the Department of Mines and Geology (Karnataka State) from 1974 to 2007 in a shallow observation well located outside the forest zone 20 km east of the study site. Although at the annual scale the observation well is much more reactive than P10, they display a very similar long-term trend. This observation suggests that the model was able to describe reasonably the global long-term behaviour of the groundwater.

Figure 9 : Simulated variations of water table level (in masl) in piezometer P10 (black line, left Y-axis) and water level (depth to ground level in meters) recorded by Department of Mines and Geology from 1974 to 2007 in a shallow observation well located outside the forest zone 20 km east of the study site (grey line with dots, right Y-axis)

Figure 10 illustrates the simulated variations of evaporation and transpiration during two years. It shows that transpiration by trees from the soil layer is the dominant flux during most of the year, especially during rainy season. Soil evapotranspiration by the understorey vegetation can be significant during dry season, depending on the occurrence of isolated rainy events. Transpiration of water from the deep weathered zone occurs mainly during dry season, and during dry periods on the course of the monsoon season. Because the model computes transpiration successively from soil and then from the weathered zone, the latter can occur only when soil water is completely depleted, leading to abrupt alternances between the two fluxes (figure 10c), which are probably much smoother in reality.

Figure 10: Example of simulated daily evapotranspiration fluxes (in mm.day^{-1}) compared to PET during two years a) variations of LAI b) Ein and Eu c) Ts and Twz (see text for signification of abbreviations)

With an objective to obtain an assessment of the water balance at the watershed scale, we need to assess the representativity of the monitored piezometers with respect to the entire area. The parameter $WZMD_{max}$, which is driving the most important part of the observed piezometer variability, is probably linked with the regolith depth in the vicinity of the piezometer. P10 is located in an area where the regolith depth is around 8m, P3 around 15 m and P6 more than 20m. A resistivity logging performed on P5 suggested a regolith depth of 22m (Braun et al., 2008). As a first approach, we can consider that P10, P3 and P5 are representative of area with regolith depth of 0-12m, 12-18m and more than 18m respectively. According to the regolith depth distribution in the watershed (Figure 2), the proportion is 30%, 27% and 43% for P10, P3 and P5 respectively. With this hypothesis, the watershed balance (Table 3) appears roughly equilibrated during the 32 years simulation period, while the water gain was 125 mm.year^{-1} during the monitoring period. The average water uptake by trees from the deep weathered zone is 104 mm, and average groundwater underflow is 78 mm.year^{-1}. Groundwater recharge is equivalent to underflow on the long term. This value is close to the recharge that was assessed in this area with Chloride mass balance method (45 mm.year^{-1}, Maréchal et al., 2009).

Discussion

The 5 years monitoring allowed us to give a tentative assessment of the water balance of a small experimental watershed using a simple conceptual lumped model. However, the

520 exercise has proven to be difficult, due to the climatic context and the presence of forest. The
521 plausibility of the model results and the future work needed to validate them are discussed in
522 this section.
523
524 One uncertainty is linked to the assessment of evapotranspiration in forest stands. This issue
525 continues to generate a great deal of controversy in the litterature (Andreassian, 2004 ;
526 Bruijnzeel, 2004 ; Robinson et al., 2003). The difficulty is also greater for regions with the
527 index of dryness (PET/Rf) close to 1.0 (Zhang et al., 2004), which is the case in our study
528 site. However, despite its limitations, the Penman-Montieth PET approach has proven its
529 ability to simulate soil water moisture in a broad range of climatic conditions and tree species
530 (Granier et al., 1999). The average total evapotranspiration found in our long term simulations
531 (around 900 mm.year^{-1}, out of which about 100 mm are linked to extra transpiration by deep
532 tree roots, see Table 3) is in very good agreement with the worldwide evapotranspiration
533 curve proposed for forests and grasslands by Zhang et al. (2001). In our climatic context,
534 water percolation towards the deep vadose zone is mainly concentrated during short rainy
535 periods of the monsoon season, usually few days to two weeks, followed by drier periods. In
536 this configuration, soil water budget is less sensitive to evapotranspiration assessment.
537 However, direct measurements of forest evapotranspiration would allow a better calibration of
538 the model.
539
540 According to our model, the spatial variability of the water reservoir located at depth in the
541 weathered zone and accessible to deep roots of trees is a key parameter for water budgeting in
542 semi-arid forested watersheds. Our calibration gave values ranging from 50 to 470 mm (Table
543 2). Few studies have been dedicated to measure the hydraulic properties of weathered granitic
544 rocks (Jones and Graham, 1993; Katsura et al., 2006). They suggest that weathered rocks have

545 the capacity to hold appreciable amount of water that is available to plants (Jones and
546 Graham, 1993 ; Williamson et al., 2004). The fact that tree roots are able to uptake water at
547 considerable depth, especially in water limited ecosystems is widely accepted (Nepstad et al.,
548 1994 ; Canadell et al., 1996 ; Collins and Bras, 2007). Importance of water storage in deep
549 weathered rock in forested ecosystems has recently gained recognition, and large scale
550 surveys to quantify deep water reservoirs have been attempted, for example in Cambodia
551 (Ohnuki et al., 2008), leading to estimates as high as 1350 mm. The average total porosity of
552 the saprolite in the Mule Hole watershed was estimated at 12% from geophysical and
553 geochemical studies (Braun et al., 2008). Even assuming that the proportion of the porosity
554 available to plants is only 5%, considering a 16 m deep saprolite would lead to an average
555 water storage capacity of 800 mm, which is compatible with our findings. Considerable
556 spatial variability of water stress and tree mortality during drought period is commonly
557 reported in dry deciduous forests (Nath et al., 2006). A survey dedicated to check whether
558 part of this variability can be explained by the regolith depth would constitute a validation of
559 our hypothesis.
560
561 The most surprising consequence of the model calibration is the great importance of the
562 recharge reservoir, and its low recession coefficient. In temperate regions, recharge process is
563 usually considered to be very quick, and in most models water percolated below the soil zone
564 is immediately transferred to the groundwater. This is acceptable because groundwater table is
565 generally shallow, and the regolith matric porosity is filled every year by recharge. However,
566 the fact that matric water can drain for a long time is well documented (Healy and Cook,
567 2002). In a chalk aquifer, Price et al. (2000) demonstrated that the delay between recharge
568 period and the smooth water table rise can be explained by matric water storage in the vadose
569 zone, which is slowly released to groundwater during dry periods. By monitoring water

570 content variations in a 21m deep sandstone vadose zone, Rimon et al. (2007) found a
571 variation of 660 mm of water content during a rainy season, and a slow decrease in water
572 content during the dry season. In a hydrogologic survey in Australia, in a granitic
573 environment, Ghauri (2004) observes a long delay between rainfall and groundwater
574 response, attributed to matric storage in the deep vadose zone. If this hypothesis is confirmed,
575 it could be of considerable importance for water resource evaluation in hard rock aquifers,
576 because in most cases recharge is assessed through water table level methods (Healy and
577 Cook, 2002). Monitoring of water content variations in the deep vadose zone of our
578 experimental watershed would allow validating this hypothesis.
579
580 The modelled watershed balance leads to an average water flow of about 180 mm.year^{-1}, out
581 of which 80 mm is groundwater underflow. This underflow might reach the streams of higher
582 order rivers, like Nugu Hole or Kabini (Figure 1). Indeed, it is very small compared to the
583 estimates of the flows produced in the humid zone of the climatic gradient that range from
584 900 to 4700 mm.year^{-1} (Putty and Prasad, 2000). However, these high flows are produced
585 during the rainy season, and during the dry season rivers virtually dry up (Putty and Prasad,
586 2000). Because groundwater underflow from transition area produces a fairly constant load,
587 it might be of significant importance in sustaining the baseflow in large rivers during the dry
588 season. This will be assessed through a regional modelling in a future work.
589
590 **Conclusions**
591
592 This study is based on a five years monitoring of an experimental forested watershed in the
593 South India, and using a conceptual model of the water balance over a 32 years period
594 allowed us to draw the following conclusions :

595 i) In tropical forest ecosystems, deciduous trees can uptake a significant amount of water from
596 the deep regolith. This mechanism is particularly important at the end of the dry summer
597 period, because the leaf flushing can precede monsoon rains by several weeks. More
598 investigations are needed to check if variability in regolith depth can be linked to the
599 variability of tree mortality during dry periods in monsoon season.
600 ii) This water uptake, combined with the spatial variability of regolith depth, can account for
601 the variable lag time between drainage events and groundwater rise observed for the different
602 piezometers.
603 iii) Water table response to the recharge is buffered due to the long vertical travel time
604 through the deep vadose zone, which constitutes a major water reservoir. The five years
605 monitoring period reveals that the watershed water balance is not equilibrated, mainly due to
606 large variations in water content in the vadose zone. This observation is of great importance
607 for water resource assessment, as water level fluctuation method is often used to estimate
608 yearly groundwater recharge, especially in India (G.E.C., 1997). Our results show that this
609 method can lead to an underestimation of recharge when vadose zone is large.
610
611 This study stresses the importance of long term observatories for the understanding of the
612 hydrological processes in tropical forested ecosystems.
613

614 **Acknowledgements**

615 The Mule Hole basin is part of the ORE-BVET project (Observatoire de Recherche en
616 Environnement – Bassin Versant Expérimentaux Tropicaux, www.orebvet.fr). Apart from the
617 specific support from the French Institute of Research for Development (IRD), the Embassy
618 of France in India and the Indian Institute of Science, our project benefited of funding from
619 IRD and INSU/CNRS (Institut National des Sciences de l'Univers / Centre National de la

Recherche Scientifique) through the French programmes ECCO-PNRH (Ecosphère Continentale: Processus et Modélisation – Programme National Recherche Hydrologique), EC2CO (Ecosphère Continentale et Côtière) and ACI-Eau. It is also funded by the Indo-French programme IFCPAR (Indo-French Center for the Promotion of Advanced Research W-3000). The multidisciplinary research carried on the Mule Hole watershed began in 2002 under the control of the IFCWS (Indo-French Cell for Water Sciences), joint laboratory IISc/IRD. We thank the Department of Mines and Geology of Karnataka for providing data and the Karnataka Forest Department and the staff of the Bandipur National Park for all the facilities and support they provided.

630 **References**

631

632 Andréassian, V., 2004 Water and forests: from historical controversy to scientific debate.
633 Journal of Hydrology 291, 1-27.

634 Anuraga, T.S., Ruiz, L., Mohan Kumar, M.S., Sekhar, M. and Leijnse, T.A., 2006 Estimating
635 groundwater recharge using land use and soil data: a case study in South India.
636 Agricultural Water Management 84 (1-2) 65-76.

637 Barbiéro, L., Parate, H. R., Descloitres, M., Bost, A., Furian, S., Mohan Kumar, M.S., Kumar,
638 C., and Braun, J. J., 2007. Using a structural approach to identifyrelationships between soil
639 and erosion in a semi-humid forested area, south india. Catena 70(3), 313–329.

640 Beven, K.J., 2001. Rainfall-runoff modelling: the primer. Wiley, Chichester, 360p

641 Braun J.J., Ruiz L., Riotte J., Mohan Kumar M.S., Murari V., Sekhar M., Barbiéro L.,
642 Descloitres M., Bost A., Dupré B., Lagane C., 2005. Chemical and physical weathering in
643 the Kabini River Basin, South India. Geochimica Cosmochimica Acta 69 (10), A691-A691

644 Braun, J.J., Descloitres, M., Riotte, J., Barbiéro, L., Fleury, S., Boeglin, J.L., Ruiz, L., Muddu,
645 S., Mohan Kumar, M.S., Kumar, M.C., and Dupré, B., 2006. Regolith thickness inferred
646 from geophysical and geochemical studies in a tropical watershed developed on gneissic
647 basement: Moole Hole, Western Ghâts (South India). Geochimica et Cosmochimica Acta
648 70 (18), A65-A65

649 Braun, J.J., Descloitres, M., Riotte, J., Fleury, S., Barbiéro, L., Boeglin, J.L., Violette, A.,
650 Lacarce, E., Ruiz, L., Sekhar, M., Mohan Kumar, M.S., Subramanian, S. and Dupré, B.,
651 2008 Regolith mass balance inferred from combined mineralogical, geochemical and
652 geophysical studies: Mule Hole gneissic watershed, South India. Geochimica and
653 Cosmochimica Acta, http://dx.doi.org/10.1016/j.gca.2008.11.013

654 Bruijnzeel, L.A., 2004 Hydrological functions of tropical forests: not seeing the soil for the
655 trees? Agriculture, Ecosystems & Environment, 104(1), 185-228.
656 Burnash, R.J.C., 1995. In: V.P. Singh, Editor, The NWS river forecast system—catchment
657 modeling, Computer Models of Watershed Hydrology, Water Resources Publications,
658 Highlands ranch, Co. 311–366.
659 Canadell, J., Jackson, R.B., Ehleringer, J.R., Mooney, H.A., Sala, O.E., Schulze, E.-D., 1996.
660 Maximum rooting depth of vegetation types at the global scale. Oecologia 108, 583–595
661 Collins, D. B. G. and Bras, R. L., 2007. Plant rooting strategies in water-limited ecosystems.
662 Water Resources Research 43, W06407
663 Descloitres, M., Ruiz, L., Sekhar, M., Legchenko, A., Braun, J-J., Mohan Kumar, M. S., and
664 Subramanian, S., 2008. Characterization of seasonal local recharge using electrical
665 resistivity tomography and magnetic resonance sounding. Hydrological Processes 22(3),
666 384-394.
667 De Vries, J.J., and Simmers, I., 2002. Groundwater recharge: an overview of processes and
668 challenges. Hydrogeology Journal 10, 8–15.
669 Dewandel, B., Lachassagne, P., Wyns, R., Maréchal, J.C., Krishnamurthy, N.S., 2006. A
670 generalized 3-D geological and hydrogeological conceptual model of granite aquifers
671 controlled by single or multiphase weathering. Journal of Hydrology 330 (1-2): 260-284,
672 doi:10.1016/j.jhydrol.2006.03.026.
673 Elliot, S., Baker, P.J. and Borchert, R., 2006. Leaf flushing during the dry season : the
674 paradox of Asian monsoon forests. Global ecology and biogeography 15(3), 248-257.
675 G.E.C., 1997 Groundwater Resource Estimation Methodology. Report of the Groundwater
676 Resource Estimation Committee, Ministry of Water Resources, Government of India, New
677 Delhi, India, 100 pp

678 Ghauri, S. 2004 Groundwater trends in the Central Agricultural Region. Resource
679 Management Technical Report 269. Department of Agriculture, Western Australia. 66p.
680 Granier, A., Bréda, N., Biron, P. and Vilette, S., 1999. A lumped water balance model to
681 evaluate duration and intensity of drought constraints in forest stands. Ecological
682 Modelling 116, 269-283.
683 Gunnell, Y. and Bourgeon, G., 1997. Soils and climatic geomorphology on the Karnataka
684 plateau, peninsular India. CATENA 29, 239-262.
685 Gunnell, Y., 1998. Passive margin uplifts and their influence on climatic change and
686 weathering patterns of tropical shield regions. Global and Planetary Change 18(1-2), 47-
687 57.
688 Gunnell, Y., 2000. The characterization of steady state in Earth surface systems: findings
689 from the gradient modelling of an Indian climosequence. Geomorphology 35, 11-20.
690 Healy, R.W. and Cook, P.G., 2002. Using groundwater levels to estimate recharge.
691 Hydrogeology Journal 10(1) 91-109.
692 Ilstedt, U., Malmer, A., Verbeeten, E., Murdiyarso, D., 2007. The effect of afforestation on
693 water infiltration in the tropics: a systematic review and meta-analysis. Forest Ecology and
694 Management 251 (1–2), 45–51.
695 Jones, D.P. and Graham, R.C., 1993. Water-holding characteristics of weathered granitic rock
696 in chaparral and forest ecosystems. Soil Science Society of America Journal 57, 256-261.
697 Katsura, S., Kosugi, K., Yamamoto, N. and Mizuyama, T., 2006. Saturated and unsaturated
698 hydraulic conductivities and water retention characteristics of weathered granitic bedrock.
699 Vadose Zone Journal 5(1), 35-47.
700 Legchenko, A., Descloitres, M., Bost, A., Ruiz, L., Reddy, M., Girard, J. P., Sekhar, M.,
701 Mohan Kumar, M. S., and Braun, J.-J., 2006. Resolution of MRS applied to the
702 characterization of hard-rock aquifers. Ground Water 44, 547-554.

703 Maréchal, J. C., Dewandel, B. and Subrahmanyam, K., 2004. Use of hydraulic tests at
704 different scales to characterize fracture network properties in the weathered-fractured layer
705 of a hard rock aquifer. Water Resources Research 40, W11508.
706 Maréchal, J.C., Dewandel, B., Ahmed, S., Galeazzi, L., and Zaidi, F.K., 2006. Combined
707 estimation of specific yield and natural recharge in a semi-arid groundwater basin with
708 irrigated agriculture. Journal of Hydrology 329(1-2), 281-293.
709 Maréchal, J.C., Varma, M.R.R., Riotte, J., Vouillamoz, J.M., Mohan Kumar, M.S., Ruiz, L.,
710 Sekhar, M., Braun, J.J., 2009 Indirect and direct recharges in a tropical forested watershed:
711 Mule Hole, India. Journal of Hydrology, 364 (3-4), 272-284.
712 Moore, I.D., Coltharp, G.B. and Sloan, P.G., 1983. Predicting runoff from small Appalachian
713 watersheds. Transactions of the Kentucky Academy of Sciences (USA), 44(3/4), 135-145
714 Moyen, J.F., Martin, H. and Jayananda, M., 2001. Multi-element geochemical modeling of
715 crust-mantle interactions during late-Archean crustal growth: the Closepet Granite (South
716 India). Precambrian Research 112 (1-2), 87-105.
717 Naqvi, S. M. and Rogers, J. W., 1987. Precambrian geology of India. Clarendon Press,
718 Oxford University Press, New york.
719 Nash, J. E. and Sutcliffe, J. V., 1970. River flow forecasting through conceptual models. Part
720 I. A discussion of principles. Journal of Hydrology 10 (3) 282–290.
721 Nath, C.D., Dattaraja, H.S., Suresh, H.S., Joshi, N.V. and Sukumar, R., 2006. Patterns of tree
722 growth in relation to environmental variability in the tropical dry deciduous forest at
723 Mudumalai, southern India. Journal of Biosciences 31, 651–669.
724 Nepstad, D.C., Carvalho, C.R., Davidson, E.A., Jipp, P., Lefebvre, P., Negreiros, G.H.d., da
725 Silva, E.D., Stone, T.A., Trumbore, S. and Vieira, S., 1994. The role of deep roots in the
726 hydrological and carbon cycles of Amazonian forests and pastures. Nature 372, 666–669.

727 Ohnuki, Y., Kimhean, C., Shinomiya, Y. and Toriyama, J., 2008. Distribution and
728 characteristics of soil thickness and effects upon water storage in forested areas of
729 Cambodia. Hydrological Processes 22, 1272-1280.
730 Oudin, L., Michel, C., and Anctil, F., 2005. Which potential evapotranspiration input for a
731 lumped rainfall-runoff model? Part 1-Can rainfall-runoff models effectively handle
732 detailed potential evapotranspiration inputs? Journal of Hydrology 303, 275–289.
733 Pascal, J.P., 1982. Forest map of South India, 1/250 000 scale, sheet Mercara–Mysore.
734 Travaux Section Scientifique et Technique Institut Français de Pondichéry, hors série, vol.
735 18a.
736 Pascal, J.P., 1986. Explanatory booklet on the forest map of South India. Travaux Section
737 Scientifique et Technique Institut Français de Pondichéry, Hors Serie, vol. 18.
738 Prasad, V.K., Anuradha, E., Badinath, K.V.S., 2005. Climatic controls of vegetation vigor in
739 four contrasting forest types of India-evaluating from National Oceanic and Atmospheric
740 Administration's Advanced Very High Resolution Radiometer datasets (1990–2000).
741 International Journal of Biometeorology 50, 6–16.
742 Prasad, S.N. and Hedge, M., 1986. Phenology and seasonality in the tropical deciduous forest
743 of Bandipur, South India. Proceedings of the Indian Academy of Sciences (Plant Sci.)
744 96(2), 121-133.
745 Price, M., Low, R. G., and McCann, C., 2000. Mechanisms of water storage and flow in the
746 unsaturated zone of the Chalk aquifer. Journal of Hydrology 233(1-4), 54-71.
747 Putty, M.R.Y. and Prasad, R., 2000. Understanding runoff processes using a watershed model
748 - a case study in the Western Ghats in South India. Journal of Hydrology 228, 215-227.
749 Rangarajan, R., and Athavale R.N., 2000. Annual replenishable ground water potential of
750 India - an estimate based on injected tritium studies. Journal of Hydrology, 234(1-2), 38-
751 53.

752 Rimon, Y., Dahan, O., Nativ, R. and Geyer S., 2007. Water percolation through the deep
753 vadose zone and groundwater recharge: Preliminary results based on a new vadose zone
754 monitoring system. Water Resources Research 43, W05402.
755 Robinson, M., Cognard-Plancq, A. -L., Cosandey, C., David, J., Durand, P., Fuhrer, H. -W.,
756 Hall, R., Hendriques, M. O., Marc, V., McCarthy, R., McDonnell, M., Martin, C., Nisbet,
757 T., O'Dea, P., Rodgers, M. and Zollner, A., 2003. Studies of the impact of forests on peak
758 flows and baseflows: a European perspective. Forest Ecology and Management 186(1-3),
759 85-97.
760 Rutter, A.J., 1967. An analysis of evaporation from a stand of Scots pine. In: Sopper, W.E.,
761 Lull, H.W. (Eds.), Forest Hydrology. Pergamon Press, Oxford.
762 Scanlon, B.R., Healy, R.W. and Cook, P.G., 2002 Choosing appropriate techniques for
763 quantifying groundwater recharge. Hydrogeology Journal 10(1) 18-39.
764 Scanlon, B.R., Keese, KE., Flint, AL., Flint, L E., Gaye, CB., Edmunds, W. M, and Simmers,
765 I., 2006. Global synthesis of groundwater recharge in semiarid and arid regions.
766 Hydrological Processes 20(15), 3335-3370.
767 Sekhar, M. and Ruiz, L., 2006. Regional Groundwater Modeling: A Case study of Gundal
768 sub-basin, Karnataka, India. In Krishnaswamy, J., Lele, S. and Jayakumar, R. (Eds.)
769 Hydrology and Watershed Services in the Western Ghats of India: Effects of land use and
770 land cover change. Tata-McGraw-Hill, New Delhi, India. 81-103.
771 Sekhar, M., Rasmi, S.N., Sivapullaia, P.V. and Ruiz, L., 2004. Groundwater flow modeling of
772 Gundal sub-basin in Kabini river basin, India. Asian Journal of Water Environmental
773 Pollution 1 (1–2), 65–77.
774 Sekhar, M., Mohan Kumar, M.S. and Sridharan, K., 1994. Parameter estimation in an
775 anisotropic leaky aquifer system. Journal of Hydrology 163, 373-391.

776 Shadakshara Swamy, N., Jayananda, M., and Janardhan, A. S., 1995. Geochemistry of
777 Gundlupet gneisses, Southern Karnataka: a 2.5 Ga old reworked sialic crust. In: Yoshida,
778 M., Santosh, M., and Rao, A. T. Eds.), India as a fragment of East Gondwana. Gondwana
779 Research Group.
780 Singh, K.P. and Kushwaha, C.P., 2005. Emerging paradigms of tree phenology in dry tropics.
781 Current Science 89(6) 964-975.
782 Sundarapandian, S.M., Chandrasekaran, S. and Swamy, P.S., 2005. Phenological behaviour of
783 selected tree species in tropical forest at Kodayar in te Western Ghats, Tamil Nadu, India.
784 Current Science 88(5) 805-810.
785 UNESCO, 1979. Map of the world distribution of arid regions, 54 pp, UNESCO, Paris.
786 Wagener, T., Wheater H.S. and Gupta, H.V., 2004. Rainfall-runoff Modelling in Gauged and
787 Ungauged Catchments. Imperial College Press, London, 300p
788 Ward, R.C. and Robinson, M., 2000. Principles of hydrology. McGraw-Hill, London (4th
789 edition), 450p.
790 Williamson, T.N., Newman, B.D., Graham, R.C. and Shouse, P.J., 2004. Regolith water in
791 zero-order chaparral and perennial grass watersheds four decades after vegetation
792 conversion. Vadose Zone Journal 3(3),1007-1016.
793 Wyns, R., Baltassat, J.M., Lachassagne, P., Legchenko, A., Vairon, J. and Mathieu, F., 2004.
794 Application of proton magnetic resonance soundings to groundwater reserve mapping in
795 weathered basement rocks (Brittany, France). Bulletin de la Société Géologique de France
796 175(1), 21-34.
797 Zhang, L., Dawes, W. R., and Walker, G. R., 2001. Response of mean annual
798 evapotranspiration to vegetation changes at catchment scale. Water Resources Research
799 37(3), 701–708.

800 Zhang, L., Hickel, K., Dawes, W. R., Chiew, F. H. S., Western, A. W. and Briggs, P. R.,
801 2004. A rational function approach for estimating mean annual evapotranspiration. Water
802 Resources Research 40, W02502, doi:10.1029/2003WR002710.

803 List of Figures:

804

805 Figure 1: Location map of the experimental site

806

807 Figure 2 : distribution of regolith depth across the Mule Hole watershed (from a geophysical
808 and geochemical survey by Braun et al., 2008)

809

810 Figure 3 : A schematic representation of the model COMFORT

811

812 Figure 4: a) daily forest LAI and coefficient of extinction ε, b) average monthly rainfall (Rf)
813 (1976-2007) and PET (2003-2007). Vertical bars indicate standard deviation of Rf.

814

815 Figure 5: observed (black line) and simulated (grey line) daily surface runoff (Qs in $mm.day^{-1}$)
816 at the Mule Hole watershed outlet for the 5 years of monitoring. Secondary axis is daily
817 rainfall (Rf) in mm.

818

819 Figure 6 : relative variation of water table level in hillslope piezometer, compared to
820 simulated potential recharge. Reference values for water table depth are 16.8 m, 27.8 m, 39.1
821 m and 37.4 m for P10, P3, P5 and P6 respectively.

822

823 Figure 7: observed (dots) and simulated (lines) water level (in meter above sea level) in
824 piezometer P3, P5 and P10 for the monitoring period.

825

826 Figure 8 : simulated variations of water table level (in masl) in piezometer P3, P5 and P10 for
827 the 32 year simulation period (lines). Dots represent observed values.

828

829 Figure 9 : simulated variations of water table level (in masl) in piezometer P10 (black line,
830 left Y-axis) and water level (depth to ground level in meters))recorded by Central
831 Groundwater Board from 1974 to 2007 in a shallow observation well located in an
832 agricultural zone 20 km east of the study site (grey line with dots, right Y-axis)

833

834 Figure 10: example of simulated daily evapotranspiration fluxes (in $mm.day^{-1}$) compared to
835 PET during two years a) variations of LAI ; b) Ein and Eu ; c) Ts and Twz (see text for
836 signification of abbreviations)

837

838 List of tables :

839

840 Table 1 : Soil water balance ($mm.year^{-1}$) for the monitored year and yearly average for the
841 monitored period and the whole 32 year simulated period. Signification of terms is in the text.
842 *2003-2006 average

843

844 Table 2 : model parameters for the 3 simulated piezometers.

845

846 Table 3: watershed balance components (in $mm.year^{-1}$) for the piezometers P10, P3 and P5,
847 for the monitoring period and the 32 year simulation and average watershed balance
848 components calculated by weighted average (see text).

849

Figure 1

Click here to download high resolution image

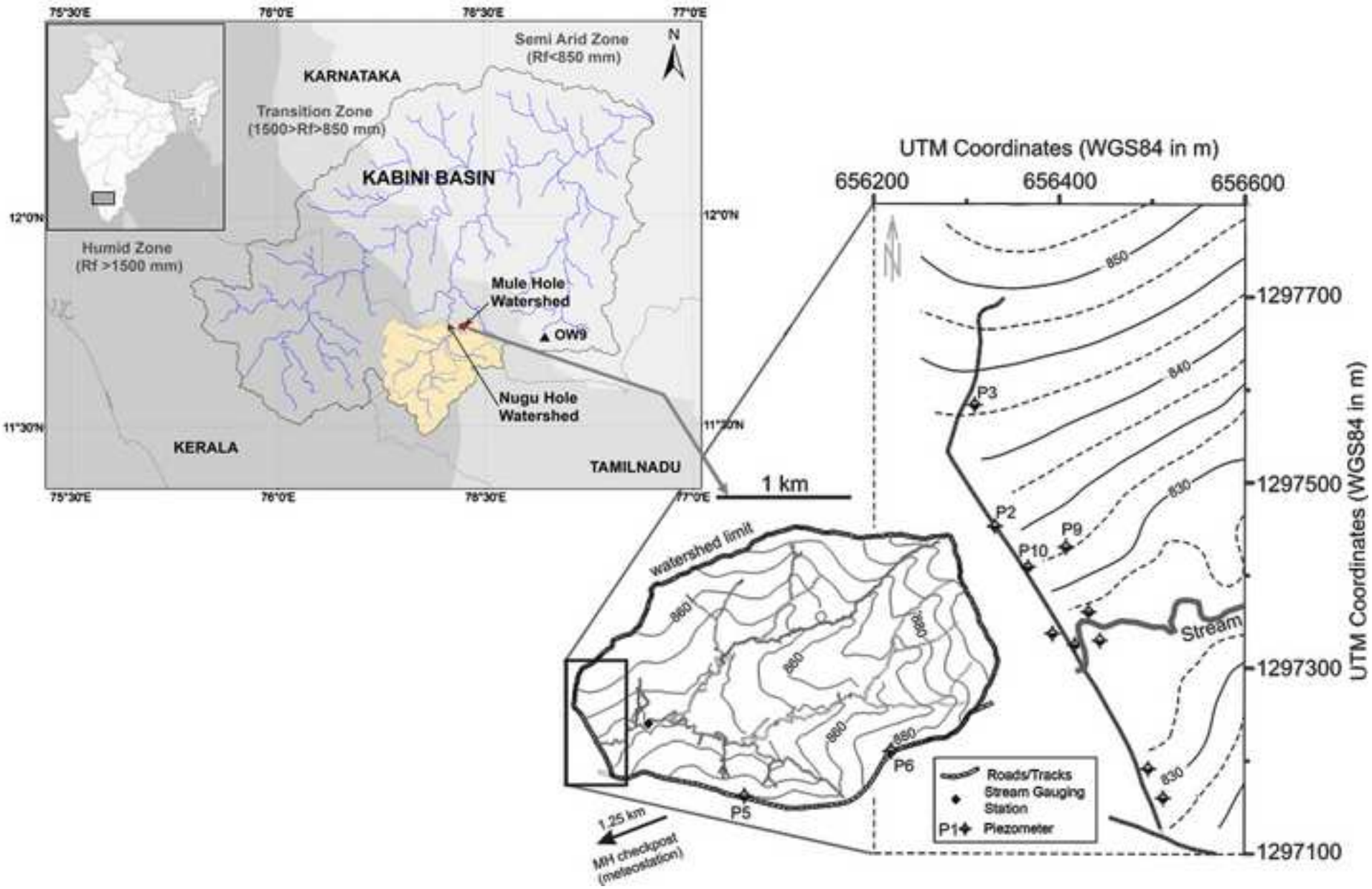

Figure 2

Click here to download high resolution image

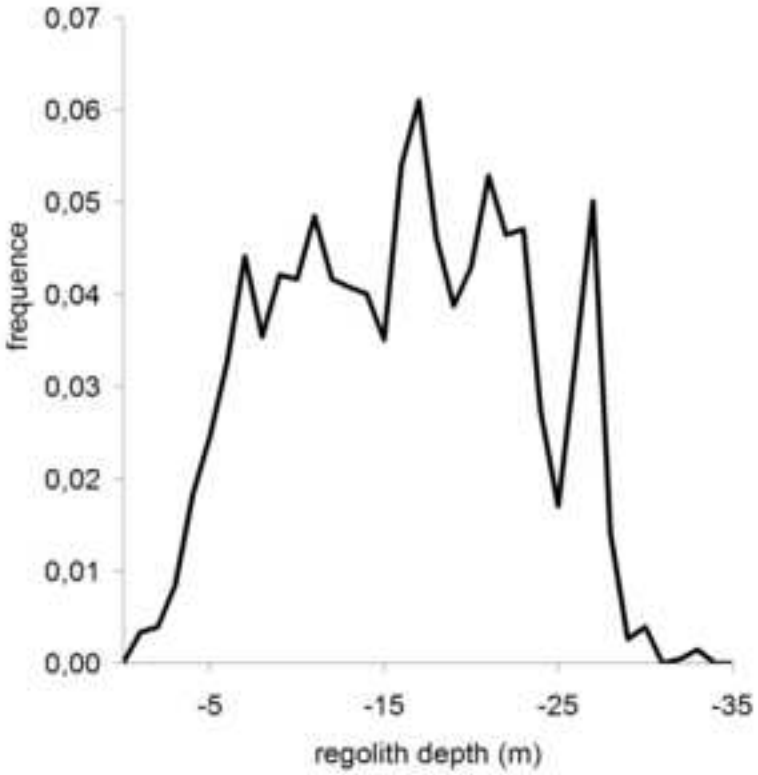

Figure 3

Click here to download high resolution image

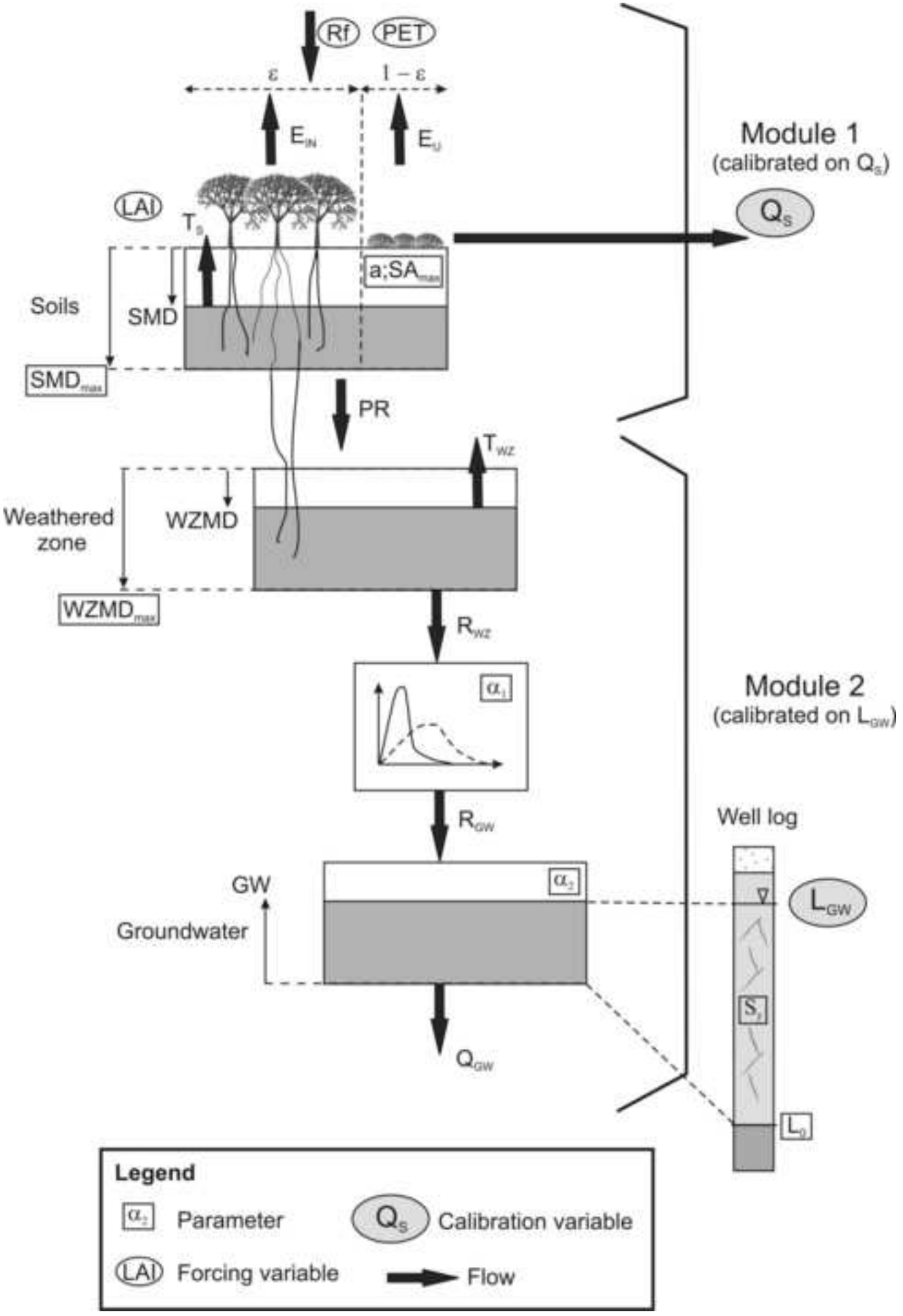

Figure 4

Click here to download high resolution image

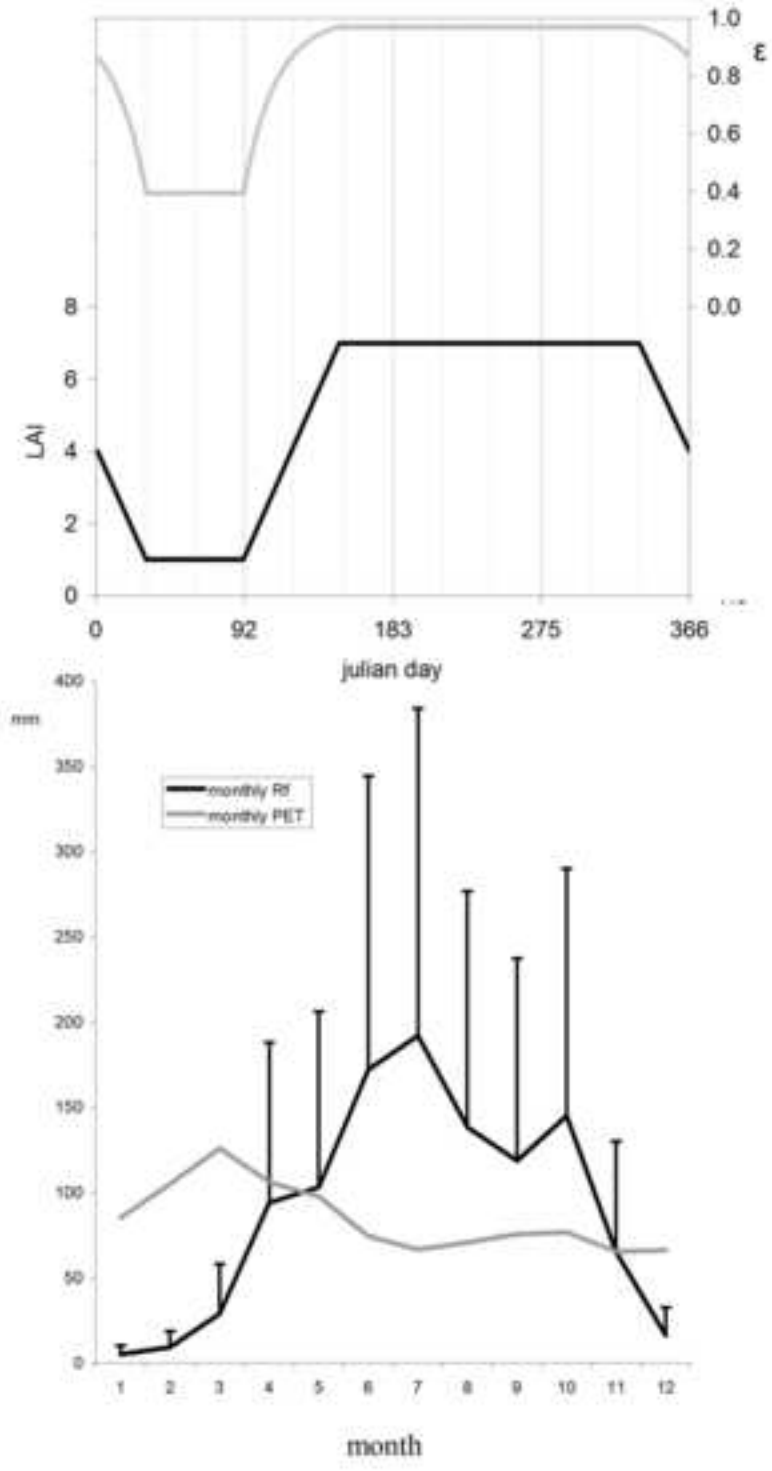

Figure 5

Click here to download high resolution image

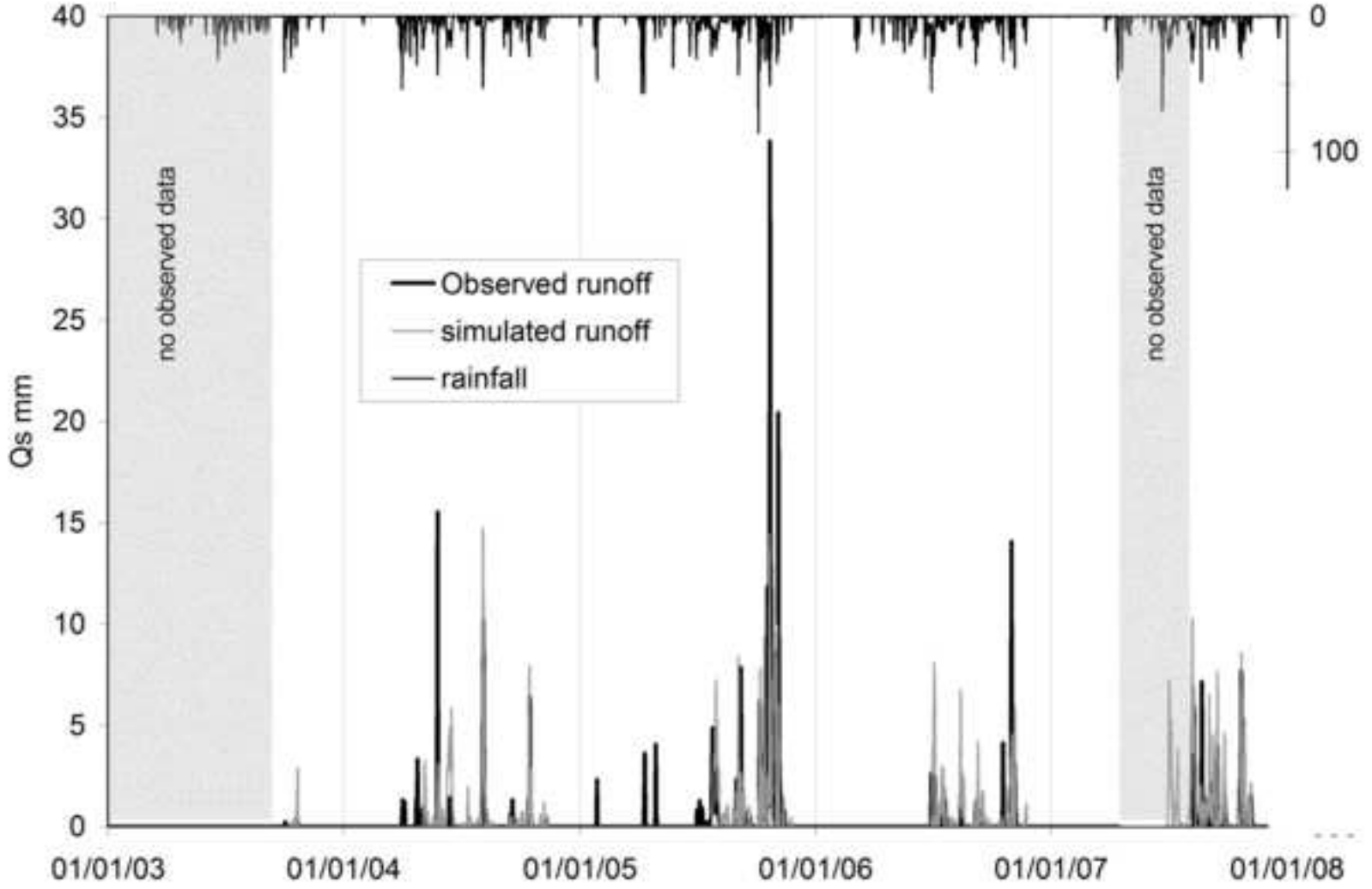

Figure 6

Click here to download high resolution image

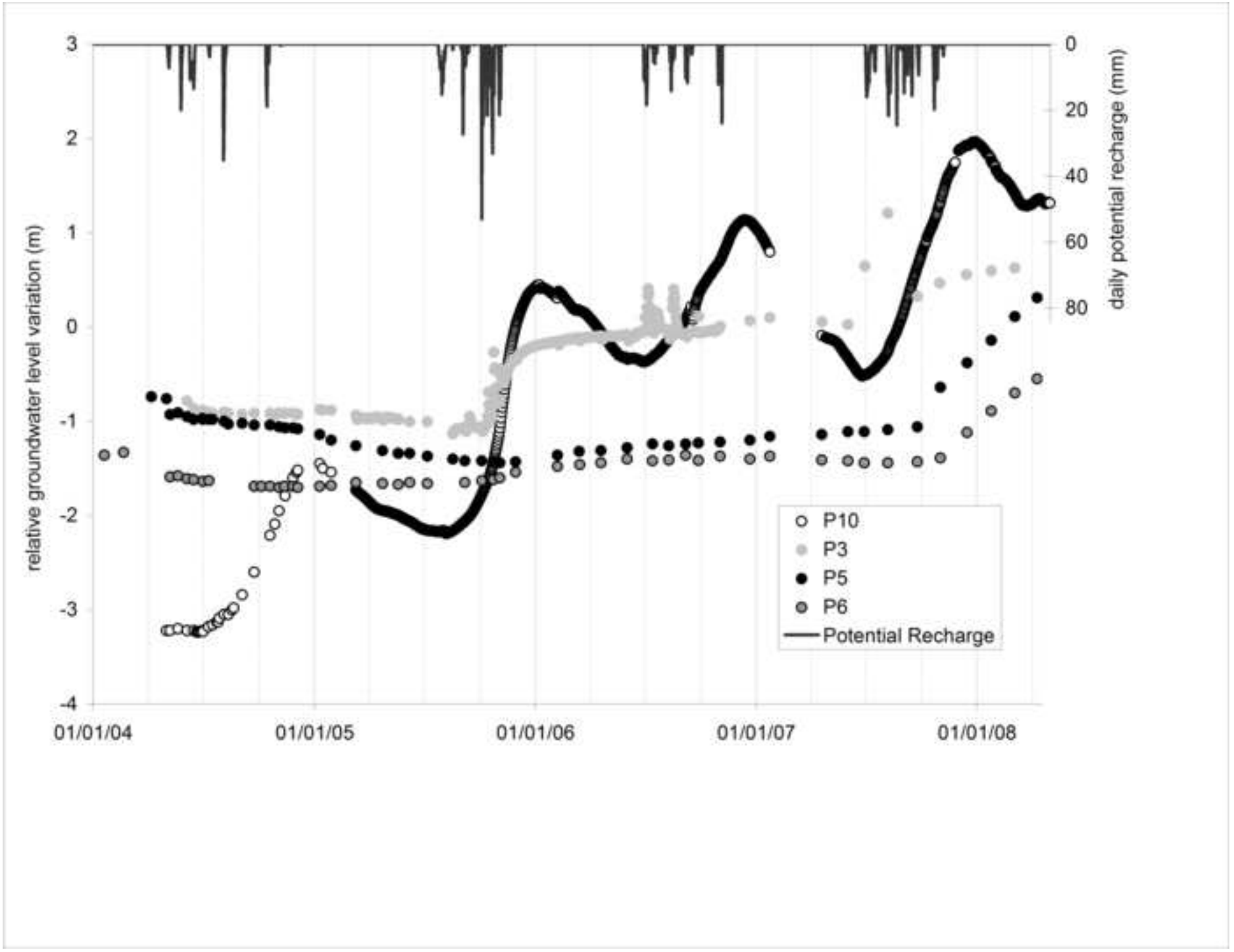

Figure 7

Click here to download high resolution image

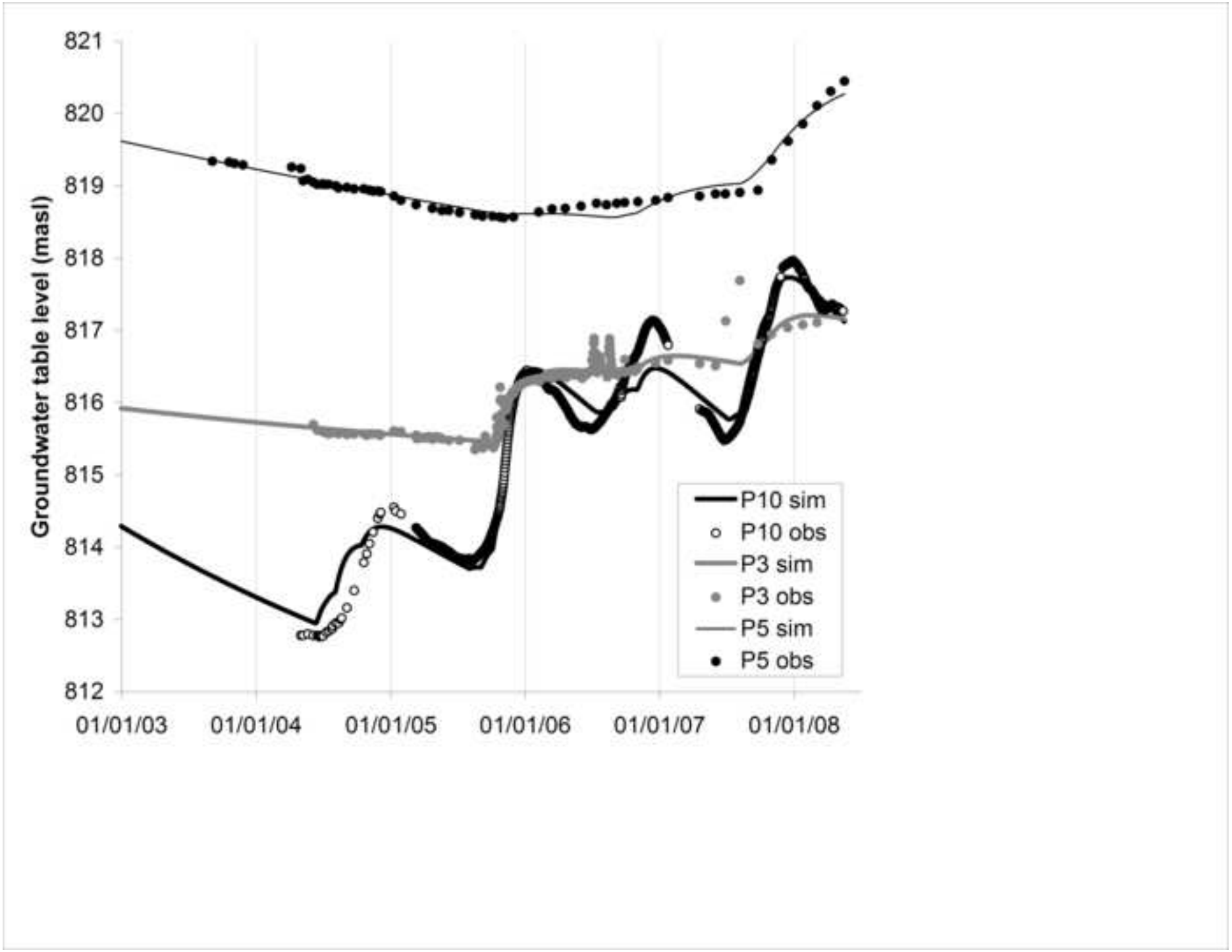

Figure 8

Click here to download high resolution image

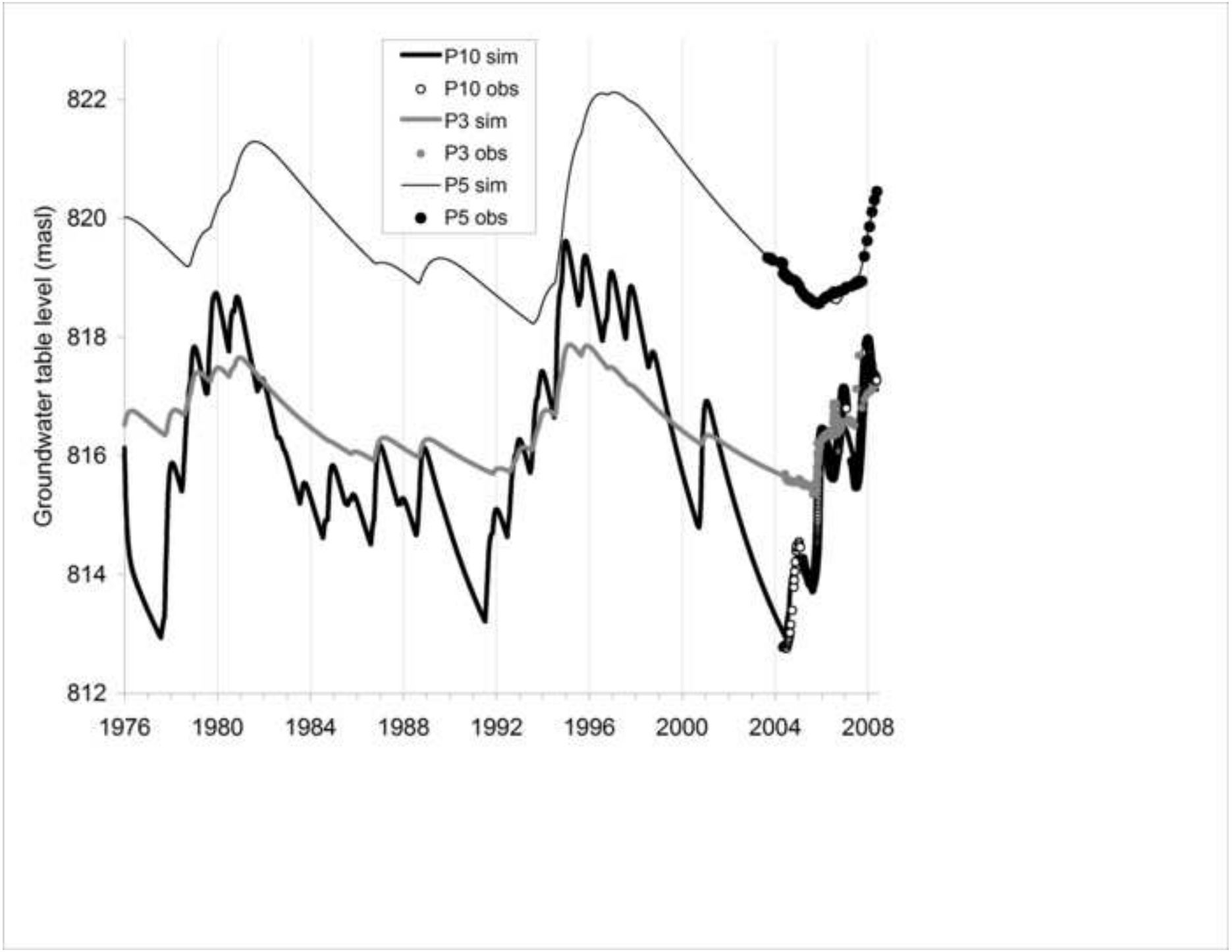

Figure 9

Click here to download high resolution image

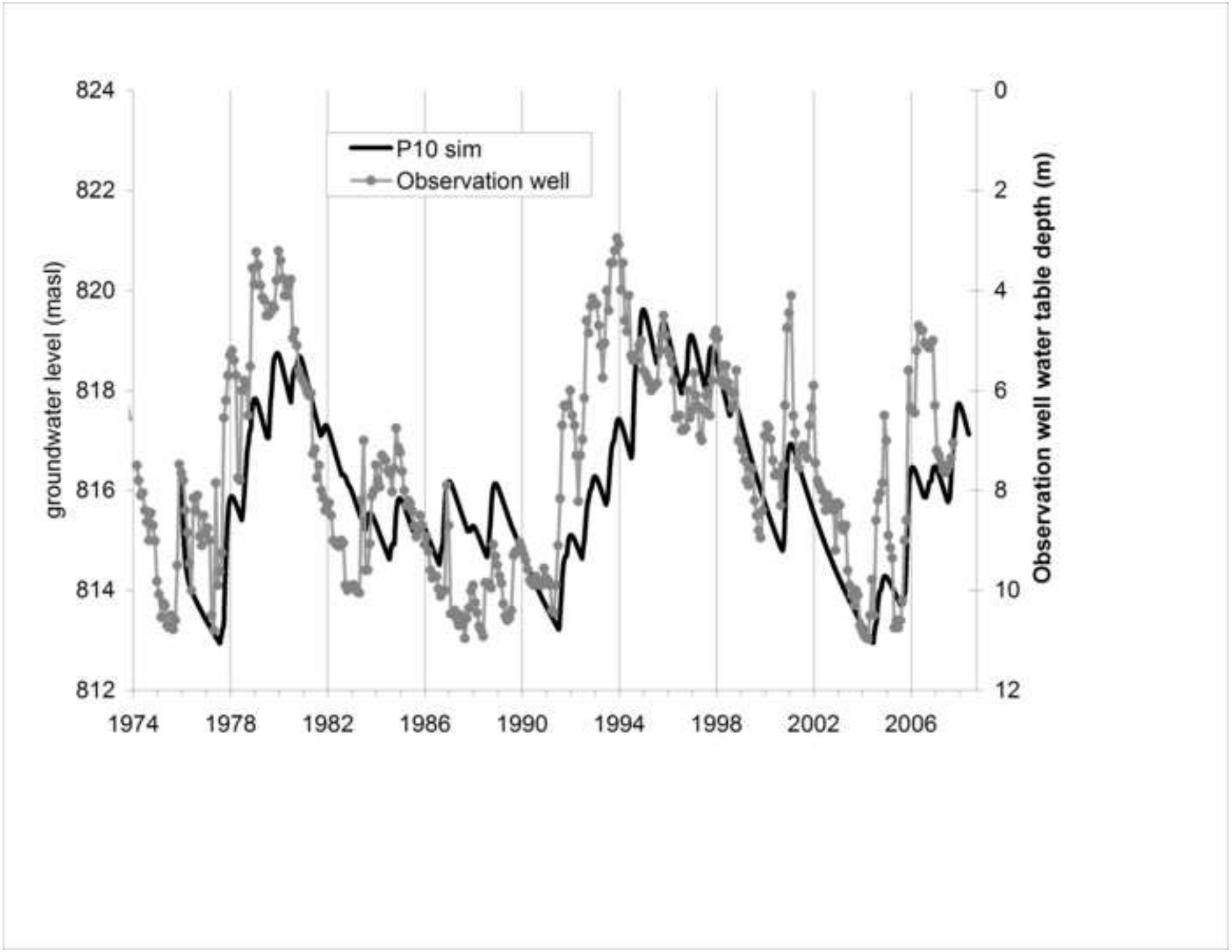

Figure 10

Click here to download high resolution image

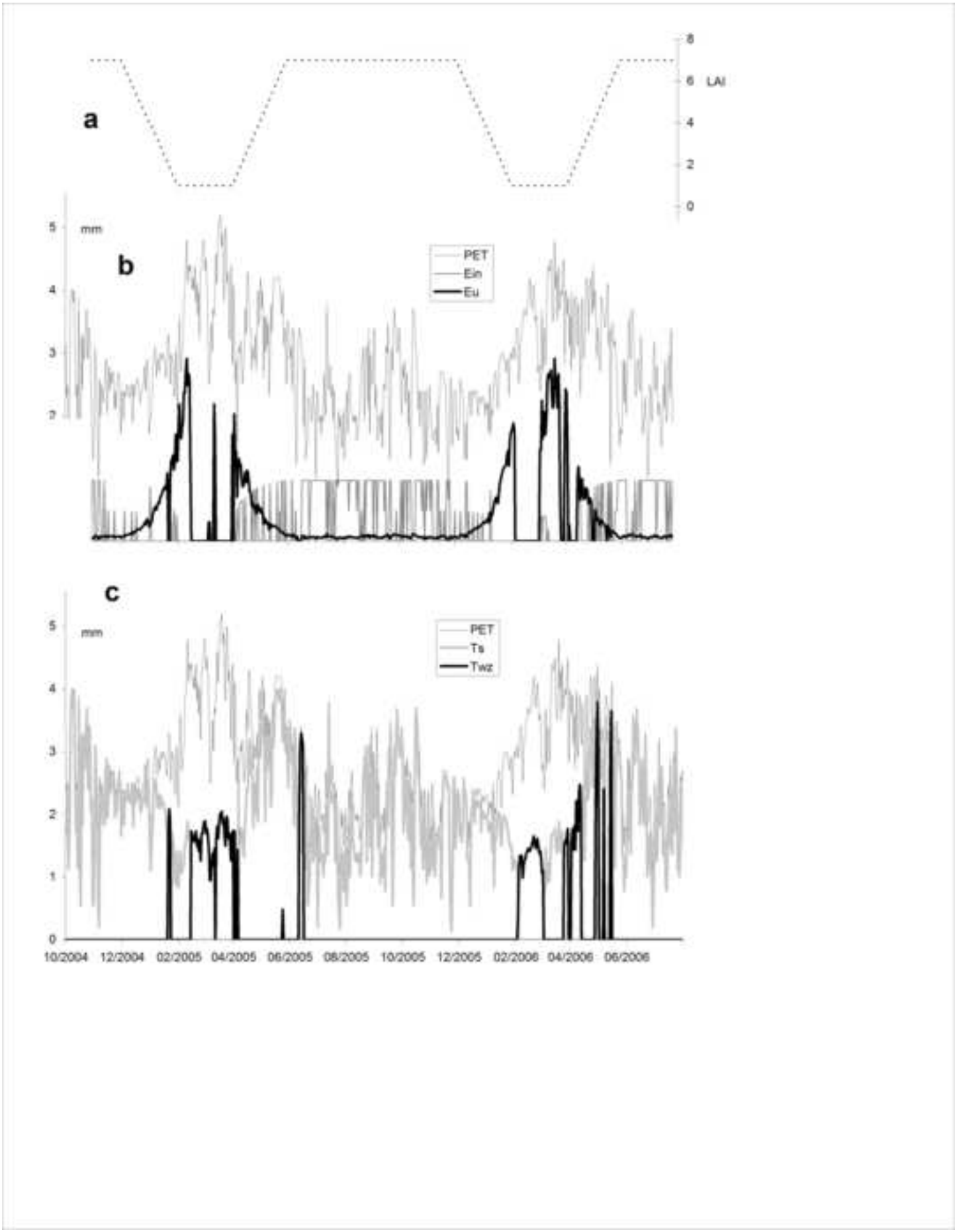

Tables

Click here to download Table: Mule Hole water balance tables 18_02_2009.pdf

	2003	2004	2005	2006	2007	2003-2007	cv %	1976-2007	cv %
Rf	706	1216	1434	1170	1252	1155	*(23)*	1091	*(32)*
PET	1101	1074	1017	1012	963	1034	*(5)*	1067	-
E_{in}	78	130	133	123	136	120	*(20)*	98	*(23)*
E_u	53	79	111	127	72	89	*(34)*	82	*(33)*
T_s	555	627	624	649	546	600	*(8)*	624	*(11)*
AET_s	686	837	868	900	754	809	*(11)*	803	*(14)*
PR	6	225	372	183	318	221	*(64)*	197	*(87)*
PET_{WZ}	268	144	97	87	118	143	*(51)*	158	*(58)*
Obs Qs	1	66	196	52	-	79 *	*(105)*	-	-
sim Qs	5	117	154	92	162	93 *	*(68)*	94	*(79)*

Table 1 : Soil water balance (mm/year) for the monitored year and yearly average for the monitored period and the whole 32 year simulated period. Signification of terms is in the text. *2003-2006 average

	P10	P3	P5
Ground level (masl)	832.82	844.24	859.14
initial watertable depth (m)	16.82	27.75	39.14
parameters:			
L_0	809.93	814.73	814.85
$WZMD_{max}$	50	250	470
α_1	$6.96\ 10^{-4}$	$4.89\ 10^{-4}$	$2.32\ 10^{-4}$
Sy	$2.10\ 10^{-3}$	$6\ 10^{-3}$	$5.11\ 10^{-3}$
α_2	$3.03\ 10^{-2}$	$1.71\ 10^{-2}$	$4.39\ 10^{-3}$

Table 2 : model parameters for the 3 simulated piezometers.

	2003-2007	cv %	1976-2007	cv %
Rf	**1155**	*(23)*	**1091**	*(32)*
AET_s	809	*(11)*	803	*(14)*
sim Qs	107	*(59)*	94	*(79)*
Local balance				
P10 T_{WZ}	31	*(83)*	43	*(52)*
P10 Q_{GW}	115	*(28)*	141	*(26)*
P3 T_{WZ}	62	*(89)*	114	*(53)*
P3 Q_{GW}	49	*(38)*	68	*(35)*
P5 T_{WZ}	62	*(89)*	141	*(47)*
P5 Q_{GW}	34	*(8)*	42	*(22)*
Watershed balance				
T_{WZ}	**53**	*(88)*	**104**	*(43)*
Q_{GW}	**62**	*(23)*	**78**	*(26)*
water balance	**125**	*(103)*	**12**	*(1346)*

Table 3: watershed balance components (in mm/year) for the piezometers P10, P3 and P5, for the monitoring period and the 31 year simulation and average watershed balance components.